Rock and Soil Mechanics

Volume 44 | Issue 6 Article 3

10-3-2023

Experimental study on the mechanical response of buried pipelines under different subsidence patterns

Yu ZHANG
College of Pipeline and Civil Engineering, China University of Petroleum (East China), Qingdao, Shandong 266580, China, zhangyu@upc.edu.cn

Hao LIANG
College of Pipeline and Civil Engineering, China University of Petroleum (East China), Qingdao, Shandong 266580, China, 1072139393@qq.com

Liang LIN
Qingdao Fusion Bridgehead Development Co., Ltd., Qingdao, Shandong 266500, China

You ZHOU
Qingdao Fusion Bridgehead Development Co., Ltd., Qingdao, Shandong 266500, China

See next page for additional authors

Experimental study on the mechanical response of buried pipelines under different subsidence patterns

Authors

Yu ZHANG, Hao LIANG, Liang LIN, You ZHOU, and Qing-song ZHAO

Rock and Soil Mechanics 2023 44(6): 1645−1656 ISSN 1000−7598
https: //doi.org/10.16285/j.rsm.2022.5983 http://rocksoilmech.researchcommons.org/journal

Experimental study on the mechanical response of buried pipelines under different subsidence patterns

ZHANG Yu[1], LIANG Hao[1], LIN Liang[2], ZHOU You[2], ZHAO Qing-song[3]

1. College of Pipeline and Civil Engineering, China University of Petroleum (East China), Qingdao, Shandong 266580, China

2. Qingdao Fusion Bridgehead Development Co., Ltd., Qingdao, Shandong 266500, China; 3. Chambroad Holding Group, Binzhou, Shandong 256599, China

Abstract: The frequent occurrence of buried pipeline accidents caused by the ground collapse and subsidence makes it urgent to carry out experimental studies on the mechanical response under different subsidence effects. A systematical survey of the pipeline strain, earth pressure and soil deformation was conducted considering the effects of ground subsidence and collapse. The result showed that due to the arching effect at the top of the pipeline, the strain and earth pressure firstly increased and then decreased with the extension of the collapse zone, while they increased as the subsidence zone extended during the collapse and settlement. In the subsidence and collapse zones, the pipeline along the axial direction exhibited a saddle shape with both ends convex and concave in the middle. Pipeline deformation was more significantly affected by the subsidence. When the subsidence and collapse were both 50 mm, the maximum strain at the top, bottom and middle of the pipeline increased by approximately 18.8%, 249% and 273% compared to the ground collapse, respectively. It could be seen by comparing the ratio of the increasing area to the decreasing area of earth pressure around the pipeline λ that λ in the subsidence was increased by 78% compared with that in the collapse; therefore, the pipeline was subjected to larger earth pressure during the subsidence. Based on the modified Marston calculation model, a method for predicting the vertical earth pressure during ground subsidence was proposed, and the accuracy of the method was verified using the model test results.

Keywords: pipeline; ground subsidence; soil collapse; pipeline strain; earth pressure around the pipeline

1 Introduction

Oil and gas pipelines are important infrastructure to ensure the regular operation of cities. With the rapid development of national economic construction, the density of pipeline networks has increased significantly, and they are characterized by long transport distances, large spans, and complex geological conditions along the route and are highly susceptible to damage during operation due to geological hazards[1]. Pipeline damage can bring direct or indirect secondary disasters, which will not only cause significant economic losses but also have a substantial negative social impact. The ground may collapse or subside under the influence of natural factors or engineering construction (such as rainfall, pit excavation, preloading, etc.), while most of the pipelines are buried at shallow depths, and they can buckle, crack, even fracture in the process of collapse or subsidence. When the soil is soft, the pipeline is easy to be snapped, while when the soil is hard, shear damage is easy to occur[2]. Therefore, ground collapse or subsidence has become an important factor that jeopardizes the safety of oil and gas pipelines, and the mechanical response of oil and gas pipelines in its process has gradually become a research hotspot, and the results of the research will provide an important theoretical basis for the assessment of pipeline safety.

The safety of oil and gas pipelines is closely related to the pipeline material characteristics, the type of soil around the pipeline, and the geological environment. During ground collapse or subsidence, the pipeline is slowly deformed by the vertical and lateral earth pressure around the pipeline, and elastic deformation occurs when the force is less than the minimum yield limit. The pipeline generates elastoplastic deformation when the force exceeds the minimum yield limit, the safety is reduced, and the limit state is reached. Therefore, tests of the pipeline strain and earth pressure around the pipeline are the key to studying the mechanical response characteristics of oil and gas pipelines. The physical model test has the advantage of simulating the real environment and the actual stress state and is a critical approach to study the mechanical response of pipelines. Some universities and research institutes in China have developed pipeline model test devices to simulate soil movement, which can complete tests for pipeline deformation and earth pressure around the pipeline under different settlement patterns[3−6]. For example, Wang et al.[7] conducted model tests on the ground settlement caused by tunnel excavation and the results showed that under the influence of buried pipelines, the ground was restricted by the pipeline to form a broader

Received: 28 June 2022 Accepted: 30 November 2022
This work was supported by the National Natural Science Foundation of China (51890914, 52179119), the Shandong Province Natural Science Foundation (ZR2019MEEO01) and the Provincial National Science Foundation of Shanxi (2021JM-373).
First author: ZHANG Yu, male, born in 1985, Associate Professor, mainly research interests:energy geomechanics and engineering.E-mail: zhangyu@upc.edu.cn
Corresponding author: LIANG Hao, male, born in 1994, PhD candidate, majoring in marine geotechnical engineering and land wind turbine foundation engineering. E-mail: 1072139393@qq.com

and shallower settlement zone. O'rourke et al.[8] investigated the effect of permanent site deformation on the mechanical response of buried pipelines by combining centrifugal model tests and numerical simulations, which showed that the results of model tests and numerical simulations were in good agreement and the pipeline strain was always in the elastic range during the tests. Vorster et al.[9] conducted ground settlement model tests for the pipelines with diameter-to-thickness ratios of 7, 12 and 21, and obtained the relationship between the diameter-to-thickness ratio and the pipeline deformation. Ju et al.[10] carried out buried pipeline tests in a large geotechnical tank and studied the effect of ground collapse on the buried pipelines, and the results indicated that when the width of the collapse zone exceeded 1.2 m, the pipeline tended to be damaged because the strain exceeded the safety value. Wang et al.[11] studied the stress characteristics of the pipeline under the effect of ground collapse using model tests and obtained the deformation process of the soil around the pipeline via particle image velocimetry (PIV) technique. They found that the soil could be divided into three deformation stages: stress redistribution, soil creep compression and post-collapse stabilization. Liu et al.[12] studied the mechanical response of buried steel pipelines caused by continuous collapse through model tests and numerical simulation and obtained the relationship between the deformation and stress of the pipeline and the collapse range. Wang et al.[13] investigated the pipeline deformation, damage and failure modes by numerical simulation, and the results revealed that the pipeline mainly underwent tensile deformation in the non-collapse zone and bending deformation in the collapse zone, and both the tensile and bending deformations led to the pipeline failure. Xu[14] carried out ground settlement tests in sand and clay through a self-developed pipe−soil interaction test platform and revealed the synergistic relationship of pipe−soil deformation during subsidence. Zhou et al.[15−17] carried out a full-scale ground settlement model test to investigate the pipeline deformation and earth pressure around the pipeline at different burial depths. They confirmed the existence of pipe−soil separation during the settlement process and modified the traditional Winkler elastic foundation beam theory. Liu et al.[18] developed a test system for induced ground settlement and studied the ground settlement induced by soil seepage erosion.

In summary, most of the existing studies are small-scale model tests, which fail to eliminate the influence of lateral friction resistance and thus lead to certain limitations in the results[19]; and most of the current studies are conducted for one type of ground settlement patterns, focusing more on the pipeline parameters (such as pipeline diameter, wall thickness, etc.) and backfill soil type, and have not yet compared and analyzed the influence of different settlement patterns on the pipeline and soil. Based on the above problems, this paper used a self-developed pipeline safety testing platform to carry out large scale ground collapse and subsidence model tests to investigate the soil deformation, pipeline strain and earth pressure distribution around the pipeline during the ground collapse and subsidence and to explore the influence of different settlement patterns on the mechanical response of the pipeline, with the hope that the research results could be of great reference value for guiding the pipeline design.

2 Test material and program

2.1 Safety testing platform

The self-developed pipeline safety test platform mainly consisted of 3 parts: the test box, sensing equipment and data acquisition system. The material of the test box was a high-strength steel plate (see Fig. 1), with the dimensions of 6.0 m×1.0 m×1.2 m in length×width×height. Both sides of the box were sealed by transparent tempered glass, through which the changes in the soil during the experiment could be directly observed. In the length direction, the test box was adjustable within 2.0 m in the middle and consisted of 10 movable steel plates of 1.0 m×0.2 m in length×width. Two hydraulic jacks were set under each plate for support, and the height of the jacks was adjusted to simulate ground collapse and subsidence during the test[20]. The sensing equipment included earth pressure cells and strain gauges to monitor the earth pressure around the pipeline and the pipeline deformation. The data acquisition system was composed of a data acquisition instrument and acquisition and analysis software, in which the data acquisition instrument could collect data from up to 72 measurement points simultaneously, and the acquisition and analysis software could record and treat the dynamic signals output from the sensing equipment to obtain the changes of earth pressure and strain around the pipeline. The self-developed pipeline safety test platform was a large-scale physical simulation test platform. First, the pipeline was placed inside the test box, the calibrated earth pressure cells and strain gauges were arranged around the pipeline, then the sand was backfilled into the test box, and the ground collapse or subsidence model test was carried out. The data acquisition system collected the earth pressure and strain readings at 0.5 s interval and recorded and saved the data to accurately determine earth pressure and strain around the pipeline.

2.2 Test material and sensor arrangement

The test filling soil used was sand. The particle size distribution curve displayed in Fig. 2 showed that the

particles with a diameter larger than 2 mm accounted for about 40%, and the coefficient of uniformity was C_c = 1.63, the curvature coefficient was C_u = 6.17, indicating that the sand was well-graded gravelly sand. Through lab tests, the unit weight of the sand was γ = 15.2 kN /m^3, the water content was w = 7.5%, the internal friction angle φ = 27.5°, and the cohesion was c = 0.5 kPa.

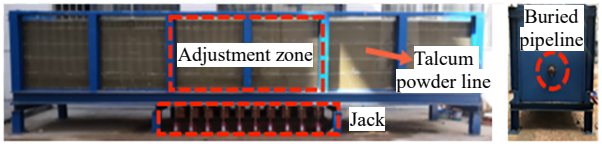

(a) Front view (b) Side view

Fig. 1 Model test box system structure

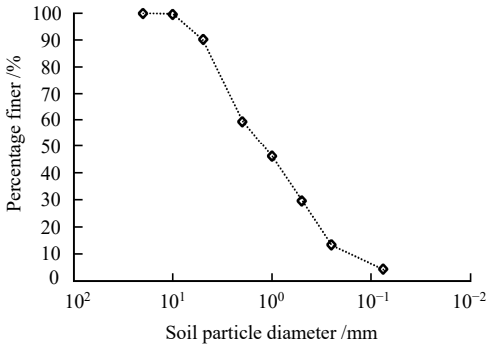

Fig. 2 Particle size distribution curve of the test sand

The pipeline was made of ordinary Q235 steel pipe, the length was 6 400 mm, the diameter was 76 mm, the wall thickness was 1.8 mm, the ratio of diameter to wall thickness was 42, the modulus of elasticity was 200 GPa and the maximum bearing capacity of pipeline was 11.13 MPa. Before the test, the pipeline was passed through a round hole reserved in the middle of the test box, and its two ends were fixed and restrained by clamps, and then the sand was backfilled into the test box to simulate the geological environment of the actual project.

Along the length direction of the pipeline, 27 earth pressure cells were symmetrically distributed in 9 sections of the pipeline, and the earth pressure cells were embedded at the top, middle and bottom of the pipeline in each section. The sensor arrangement was refined in the middle during the test. The middle position of the pipeline was taken as the symmetry axis, and the earth pressure cells were symmetrically distributed on both sides of the symmetry axis. Taking the left half section as an example, the spacing of adjacent earth pressure cells from the middle to the left edge was 400, 600, 800 and 1 200 mm (see Fig. 3). Along the length direction of the pipeline, 48 strain gauges were evenly arranged at the top, middle and bottom of the pipeline, and the spacing of adjacent strain gauges was 400 mm (see Fig. 4). To ensure that the initial state of the backfill soil was always the same, the earth pressure cell and strain gauge readings at the same location needed to be kept approximately equal before the start of each test.

2.3 Test program and procedure

The model tests were designed for ground collapse and subsidence test programs, respectively. During the backfilling, the sand was evenly layered in the test box, and the thickness of the soil layer was 0.2 m. After each layer was laid, a sand shovel was used to smooth and compact, and white talcum powder was spread on the surface to facilitate the observation of the soil settlement in the test. The above process was repeated until the filling was completed. At this time, the distance from the top of the pipeline to the surface was 0.8 m, which could meet the embedment depth requirement of oil and gas pipelines[21]. The specific test steps are as follows:

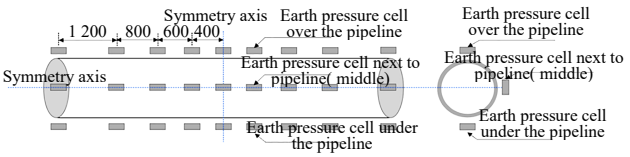

(a) Front view (b) Side view

Fig. 3 Layout of earth pressure cells (unit: mm)

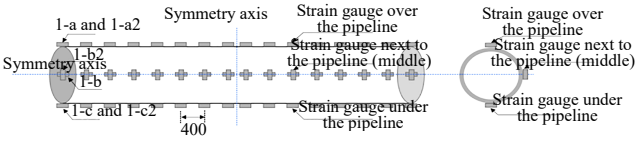

(a) Front view (b) Side view

Fig. 4 Layout of strain gauges on the pipeline (unit: mm)

(1) Ground collapse test

The test was carried out in 5 steps to adjust the 10 movable steel plates in turn (see Fig. 5). In the figure, a, b, c, d and e were respectively the positions of the movable steel plate adjusted in steps 1, 2, 3, 4 and 5. The leftmost end of the pipeline was defined as the original point of the coordinate axis, the horizontal coordinate x increased gradually along the pipeline to the right, and the center line was located at 3 m to the right of the coordinate axis origin. In the 1st step, the movable steel plates within 0.2 m on both sides (x = 2.8−3.2 m) from the center line (x = 3 m) were removed simultaneously, forming a hole with a volume of n×1.0×0.2×0.05 m^3 (n is the number of movable steel plates, and n = 2 in each adjustment step), and the next adjustment step was carried out after the soil above the steel plate freely collapsed and the monitoring data was stabilized (about 20 min). In the 2nd step, the removable steel plates within the range of −0.4−−0.2 m and 0.2−0.4 m (x = 2.6−2.8 m and x = 3.2−3.4 m) on both sides of the center line were removed. And so on until the last two removable steel plates were adjusted in the 5th step,

at which time all the movable steel plates within 1 m on the left and right sides of the center line (x = 2−4 m) were removed along the length direction of the pipeline.

(2) Ground subsidence test

The test was first carried out in 5 steps to adjust the 10 movable steel plates in turn (see Fig. 5), and in the 6th step, the 10 movable steel plates were adjusted simultaneously. In the 1st step, the movable steel plates within 0.2 m (x = 2.8 to 3.2 m) on both sides of the center line (x = 3 m) were slowly lowered by 50 mm (the subsidence volume was n×1.0×0.2×0.05 m^3) at a velocity of about 0.131 mm /s; the upper soil also settled slowly with the movable steel plates, and after the soil subsidence was stable, the next adjustment step was conducted after standing for 12 h. In the 2nd step, the movable steel plates in the range of −0.4—−0.2 m and 0.2−0.4 m (x = 2.6−2.8 m and x = 3.2−3.4 m) on both sides of the center line were lowered by 50 mm at the same time. And so on until the last two movable steel plates were adjusted in the 5th step, at this time the soil within 1 m of the left and right sides of the center line (x = 2−4 m) subsided by 50 mm integrally. In the 6th step, 10 movable steel plates were adjusted simultaneously so that all the plates were lowered by another 50 mm, at which time the soil (x = 2−4 m) subsided by a total of 100 mm.

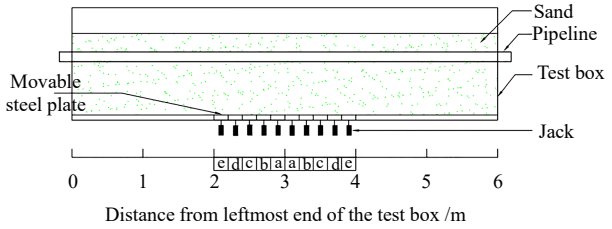

Fig. 5 Adjustment step for the movable steel plate

3 Mechanical response of pipeline due to ground collapse

3.1 Definition of collapse stage and soil deformation characteristics

In the ground collapse test, the collapse zone was a dynamically changing zone, and after the 1st step of adjustment, the collapse zone was x = 2.8−3.2 m, and the non-collapse zone was x = 0−2.8 m and x = 3.2−6 m (the leftmost end of the pipe is the original point of the coordinate axis). After the 2nd step of adjustment, the collapse zone was x = 2.6−3.4 m, and the non-collapse zone was x = 0−2.6 m and x = 3.4−6 m. And so on until the test was completed, the collapse zone was x = 2−4 m, and the non-collapse zone was x = 0−2 m and x = 4−6 m. From the literature [22], it was known that the collapse of the overlaying soil above the pipeline occurred during the ground collapse, and the mechanical properties of the pipeline changed abruptly with the collapse of the overlaying soil. Hence, it was defined as the partial collapse stage (in the 1st and 2nd steps of adjustment) when the overlaying soil was intact, and it was defined as the complete collapse stage (the 3rd to the 5th steps of adjustment) after the collapse. In the partial collapse stage, the soil below the pipeline collapsed toward the collapse zone, forming a vaulted hole. However, the overlaying soil still had integrity under the restriction of the pipeline (see Fig. 6(a)), and the vaulted hole extended toward the ground surface as the collapse zone expanded (see Fig. 6(b)). After entering the complete collapse stage, the overlaying soil collapsed due to shear failure, at which time the pipeline was suspended and a nearly vertical shear plane was formed at the edge of the collapse zone (see Fig. 6(c)). With the further expansion of the collapse zone, the soil continued to collapse towards both sides. The soil in the non-collapse zone was less affected by the collapse and did not produce significant deformation in the whole process.

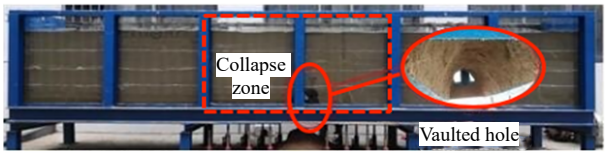

(a) Soil deformation after the 1st step of adjustment (partial collapse stage)

(b) Soil deformation after the 2nd step of adjustment (partial collapse stage)

(c) Soil deformation after the 3rd step of adjustment (complete collapse stage)

Fig. 6 Ground deformation during the collapse

3.2 Effect of ground collapse on pipeline strain

Given the symmetrical distribution of strain along the center line (see Fig. 7), the left half of the pipeline was taken in this study (x = 0−3 m). After the pipeline was buried into the soil, the compressive strain was generated by the sand confining pressure, and the strain of the buried pipeline was zeroed before the test. As shown in Figs. 7−9, when the strain at the measurement point was positive, the pipeline underwent a certain degree of rebound, and the positive strain was positively correlated with the amount of rebound, which was called tensile strain in this study. In contrast, when the strain was negative, the pipeline was further compressed, and the negative strain was negatively correlated with the amount of compression, which was

called compressive strain in this study.

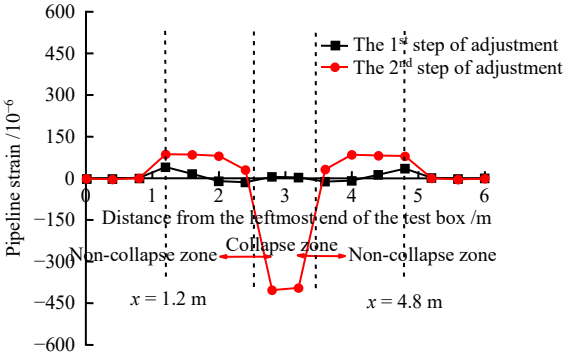

(a) Partial collapse stage

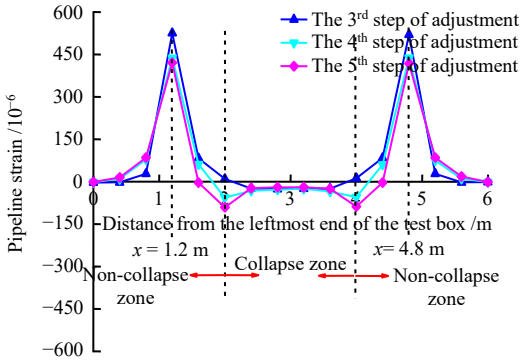

(b) Complete collapse stage

Fig. 7 Axial strain at the top of the pipeline

In the partial collapse stage (the collapse zone was x = 2.6–3 m and the non-collapse zone x = 0–2.6 m), the top of the pipeline was compressed in the collapse zone, and the compressive strain increased with the pipe length (x = 2.6 m), with the maximum value occurring at the center line (x = 3 m). In the non-collapse zone the pipeline was under tension, the tensile strain first increased and then decreased with the pipe length (x = 0 m), reaching the maximum value at x = 1.2 m (see Fig. 7(a)). In contrast, the bottom of the pipeline in the collapse zone was under tension, and the tensile strain increased with the length of the pipeline. In the non-collapsed zone the pipeline was under pressure, the compressive strain first increased and then decreased with the length of the pipeline, and the maximum compressive strain occurred at x = 2 m due to the effect of stress concentration (see Fig. 8(a)). The pipeline was considered as a simply supported beam for analysis, and the pipeline was approximately saddle-shaped with two convex sides and a concave middle along the axial direction due to the influence of ground collapse. Under the external load, the pipeline was damaged by the compressive strain exceeding the yield limit[3], so the location where the maximum compressive strain (top x = 3 m) was the critical failure plane.

After entering the complete collapse stage (collapse zone x = 2–3 m and non-collapse zone x = 0–2 m), part of the soil in the non-collapse zone moved out from the collapse zone as the overlaying soil collapsed in the collapse zone. Within the collapse zone, the compressive strain at the top of the pipeline decreased rapidly, while the tensile strain in the non-collapse zone continued to increase (see Fig. 7(b)). The area under pressure at the bottom of the pipeline kept reducing, and the maximum compressive strain gradually shifted toward the end of the pipeline (see Fig. 8(b)). Compared with the partial collapse stage, the bending deformation of the pipeline along the axial direction decreased. Therefore, large pipeline deformation occurred during the partial collapse stage, and the maximum compressive strains at the top and bottom appeared at the center of the collapse zone (x = 3 m) and x = 2 m, respectively. However, the compressive strain of the pipeline decreased and the area under pressure produced a certain degree of rebound as the overlaying soil collapsed.

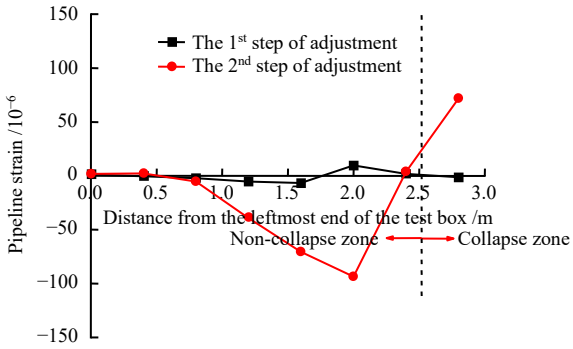

(a) Partial collapse stage

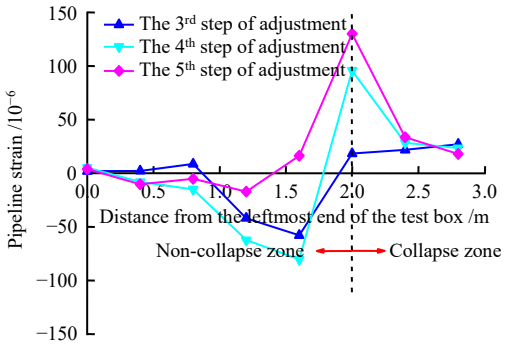

(b) Complete collapse stage

Fig. 8 Axial strain at the bottom of the pipeline

The strain in the middle of the pipeline was mainly induced by the lateral earth pressure. During the partial collapse stage, the tensile strain was generated in the middle of the pipeline, and the tensile strain increased with the increase of the pipe length. After entering the complete collapse stage, the tensile strain continued to increase in the non-collapse zone x = 0 to 1.4 m, while the tensile strain gradually decreased in other areas and converted from tensile strain to compressive strain at 1.6 m (see Fig. 9). Compared with the top and bottom of the pipeline, the collapse has less influence on the deformation of the middle part of the pipeline. Therefore,

in order to ensure the safety of the pipeline, the strength testing of the top and bottom of the buried pipeline should be strengthened in the project.

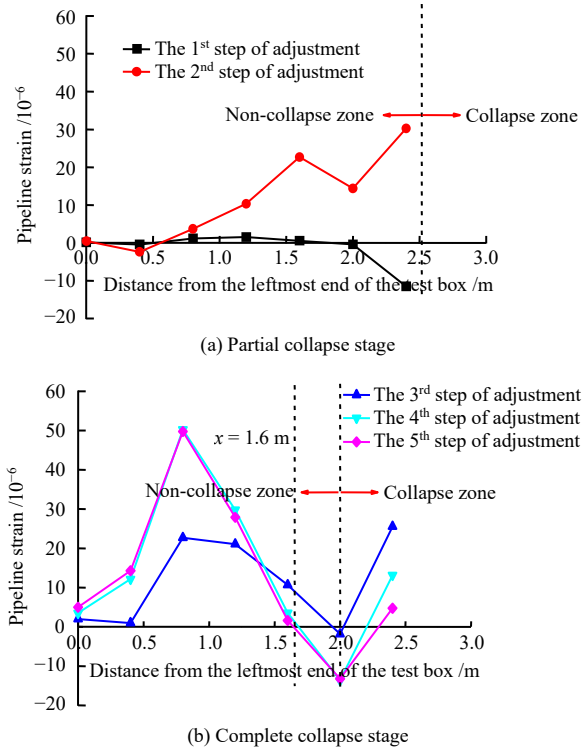

(a) Partial collapse stage

(b) Complete collapse stage

Fig. 9 Axial strain at the middle of the pipeline

3.3 Effect of ground collapse on the earth pressure around the pipeline

Before the test, the earth pressure was balanced to zero, and the measured earth pressure value minus the initial value was defined as the earth pressure increment. When the increment was positive, the earth pressure was greater than the initial value; when the increment was negative, the earth pressure was less than the initial value.

The arching effect is the main cause of pipeline failure. Before the collapse of the overlaying soil, relative movement occurred between the top of the pipeline and the outside soil. The resistance caused by friction between soil particles led to a reduction in the earth pressure of the moving soil mass and an increase in the earth pressure of the stable part[23−24]. As the earth pressure at the top of the pipeline increased, the pipeline was subjected to a positive arching effect (the top was under pressure and the bottom was under tension); while the pipeline was subjected to a negative arching effect when the earth pressure at the bottom of the pipeline increased (the top was under tension and the bottom was under pressure). In the partial collapse stage, the earth pressure increment at the top of the pipeline in the collapse zone increased with the increase of pipeline length, and the maximum value appeared at the center line (x = 3 m). The reason for this was that the overlaying soil over the pipeline was restricted by the pipeline to remain stable, while the outside soil had a tendency to move towards the collapsed hole due to its self-weight and the earth pressure above the pipeline increased sharply under the arching effect. The earth pressure in the non-collapse zone could be divided into two parts. From the initial section to 1.2 m, the effect of collapse on the earth pressure around the pipeline could be neglected. In the range of x = 1.2−2.6 m, the earth pressure was negative and the increment decreased gradually with the increase of pipeline length (see Fig. 10(a)). Stress redistribution occurred in the soil below the pipeline due to the effect of collapse, the earth pressure in the collapse zone was negative, and the increment decreased gradually with the increase of pipeline length. The earth pressure in the non-collapse zone was positive, and the increment first increased and then reduced with the increase of pipeline length, and the maximum value appeared at x = 2 m (see Fig. 11(a)). Thus, it was concluded that the pipeline was subjected to a positive arching effect in the collapse zone and a negative arching effect in the non-collapse zone. The earth pressure at each measurement point in the middle of the pipeline was negative, and the increment decreased with the increase of pipe length (see Fig. 12(a)).

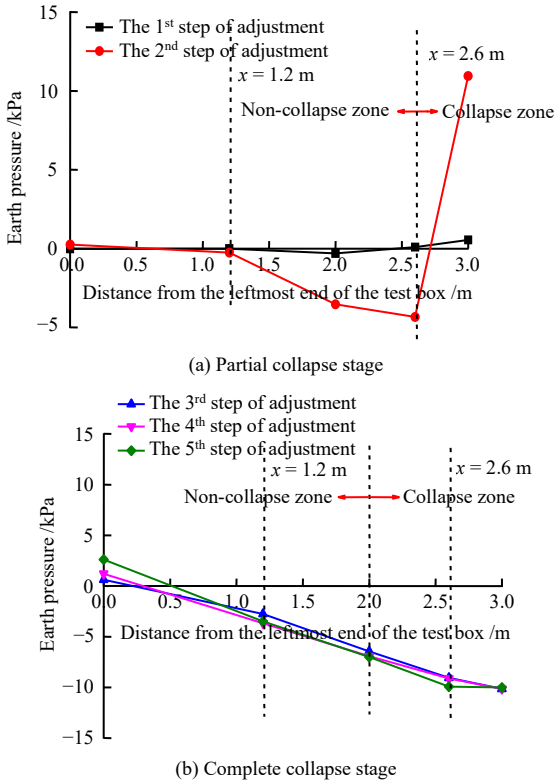

(a) Partial collapse stage

(b) Complete collapse stage

Fig. 10 Earth pressure distribution at the top of the pipeline

After entering the complete collapse stage, the earth pressure around the pipeline changed abruptly, and the upper and lower earth pressures decreased to different degrees with the increase of pipe length. In the collapse zone, the earth pressure increment above the pipeline

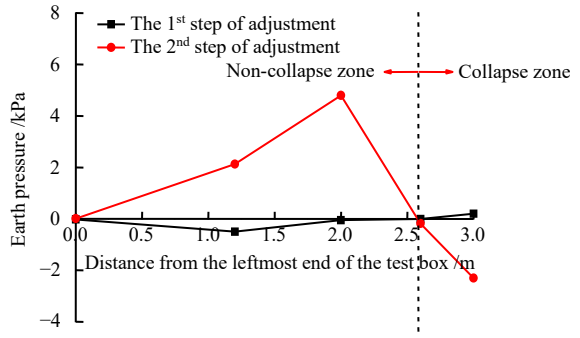

(a) Partial collapse stage

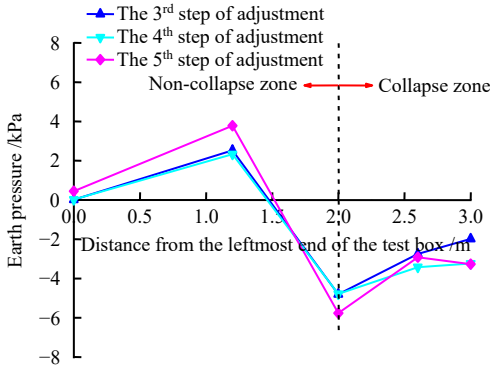

(b) Complete collapse stage

Fig. 11 Earth pressure distribution at the bottom of the pipeline

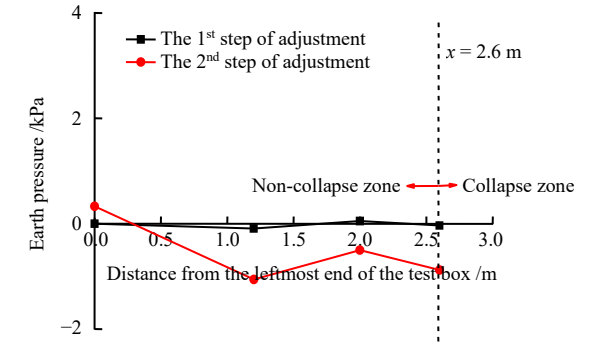

(a) Partial collapse stage

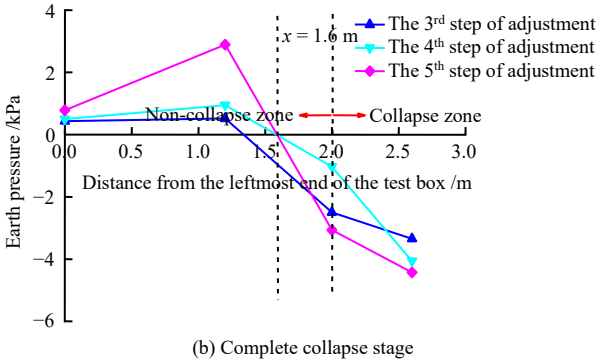

(b) Complete collapse stage

Fig. 12 Earth pressure distribution at the middle of the pipeline

changed from positive to negative because the arching effect disappeared due to the collapse of all the overlaying soil, so the earth pressure increment decreased sharply (see Fig. 10(b)). However, the earth pressure increment under the pipeline decreased from positive to negative in the range of x = 1.5−2.6 m as the soil flowed out from the collapsed hole (see Fig. 11(b)). From the left end of the pipeline to 1.6 m, the earth pressure in the middle of pipeline increased sharply due to effect of frictional resistance, and the increment turned from negative to positive, which increased first and then decreased as the pipeline length increased. In the range of x = 1.6−3.0 m, the increment of earth pressure continued to decrease as the pressure around the pipe decreased, decreasing with the increase of pipe length (see Figure 12(b)). In the range of x = 1.6−3.0 m, as the confining pressure around the pipeline reduced, the increment of earth pressure decreased continuously with the increase of pipeline length (see Fig. 12(b)). The earth pressure above and below the pipeline reached the peak values in the partial collapse stage and the maximum increments were 10.95 and 4.8 kPa, respectively. The earth pressure decreased rapidly after entering the complete collapse stage, so the pipeline was extremely vulnerable to compression failure in the partial collapse stage.

The area of the compression zone around the pipeline (the earth pressure increment was positive) was counted as A_1 and the area of the tension zone (the earth pressure increment was negative) was counted as A_2. During the ground subsidence or collapse, the ratio of A_1 to A_2 was defined as the ratio of the earth pressure around the pipeline ($\lambda = A_1/A_2$) in order to quantify the actual stress state of the pipeline. In the partial collapse stage (see Fig. 13), a sharp increase in the earth pressure ratio λ of ground above and under the pipeline, indicating a significant increase in the area of the compression zone, and then λ decreased to a stable state in the complete collapse stage. The earth pressure ratio λ within the middle (cross section) of the pipeline increased steadily with the extension of the collapse zone.

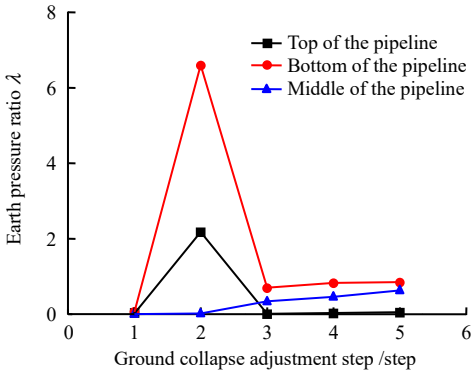

Fig. 13 Earth pressure ratio λ around the pipeline

4 Mechanical response of pipeline due to ground subsidence

4.1 Definition of subsidence stage and characteristics of soil deformation

In the subsidence test, the subsidence zone was a dynamically changing zone. After the adjustment in the

1st step, the subsidence zone was x = 2.8−3.2 m and the non-subsidence zone was x = 0−2.8 m and x = 3.2−6 m; after the adjustment in the 2nd step, the subsidence zone was x = 2.6−3.4 m and the non-subsidence zone was x = 0−2.6 m and x = 3.4−6 m. And so on until the test was finished, the subsidence zone was x = 2−4 m and the non-subsidence zone was x = 0−2 m and x = 4−6 m. The subsidence zone expansion was called the partial subsidence stage (the 1st to the 5th step of adjustment), and the subsidence displacement continued to increase until the final stabilization, which was called the complete subsidence stage (the 6th step of adjustment). In the partial subsidence stage, the soil in the subsidence zone subsided slowly from the center line to both sides as the subsidence zone extended (see Figs. 14(a) and 14(b)), and at this time, no obvious deformation occurred in the soil. In the complete subsidence stage, as the subsidence displacement continued to increase, the soil within the subsidence zone subsided sharply, and shear failure occurred at the edge of the subsidence zone, forming a sliding failure plane with an inclination of about 45° (see Fig. 14(c)). The soil in the non-subsidence zone was less affected by the subsidence effect, and there was no significant subsidence throughout the test.

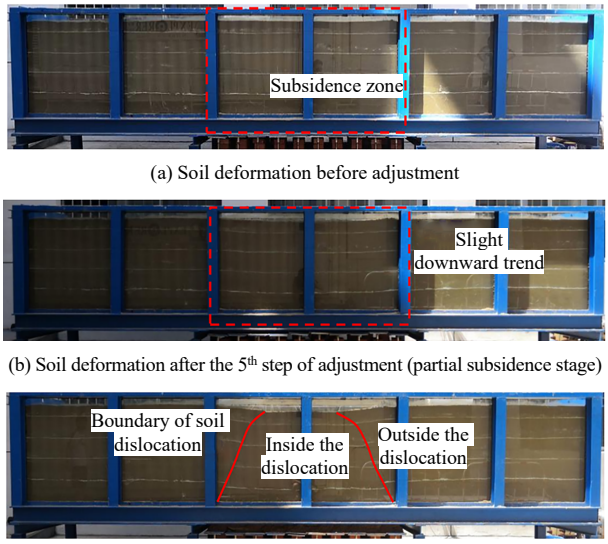

(a) Soil deformation before adjustment

(b) Soil deformation after the 5th step of adjustment (partial subsidence stage)

(c) Soil deformation after the 6th step of adjustment (complete subsidence stage)

Fig. 14 Ground deformation during the subsidence

4.2 Effect of ground subsidence on the pipeline strain

Given the symmetric distribution of strain along the center line (see Fig. 15), the left half of the pipeline was taken for study (x = 0−3 m). Figs. 15−17 show the axial strain distribution at the top, bottom, and middle of the pipeline, respectively. In the partial subsidence stage, the top and middle of the pipeline were under pressure in the subsidence zone, and the compression strain increased with the increase of the pipeline length; in the non-subsidence zone, the tensile strain increased and then decreased with the increase of the pipe length (see Figs. 15 and 17). Compared with the top and middle of the pipeline, the strain at the bottom of the pipeline exhibited an opposite distribution pattern (see Fig. 16), i.e., the tensile strain increased with the increase of the pipeline length when the pipeline was subjected to tension in the subsidence zone, and the compression strain increased and then decreased with the increase of the pipeline length when the pipeline was under pressure in the non-subsidence zone. When the pipeline was analyzed as a simple supported beam, the pipeline approximately exhibited a saddle shape with both ends convex and concave in the middle along the axial direction due to the influence of ground subsidence. The maximum compression strain at the top and middle of the pipe occurred at the center line (x = 3 m) and the maximum tensile strain was at x = 1.2 m, while the maximum

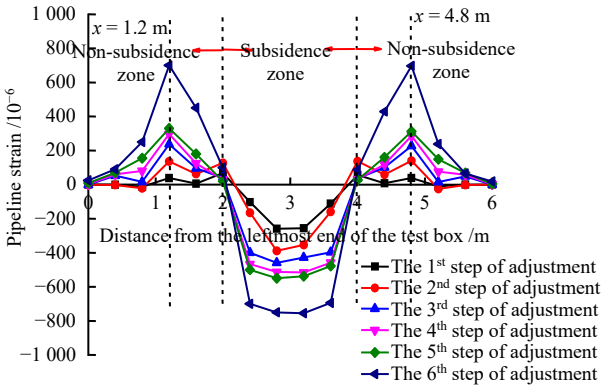

Fig. 15 Axial strain at the top of the pipeline

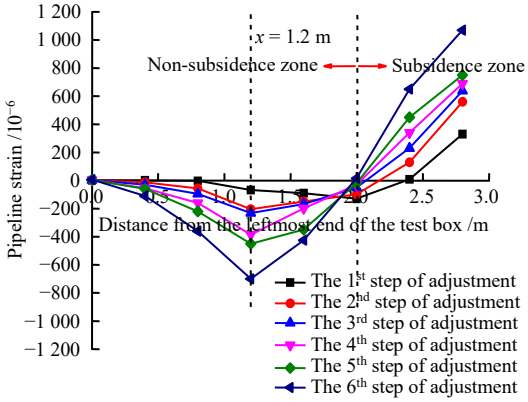

Fig. 16 Axial strain at the bottom of the pipeline

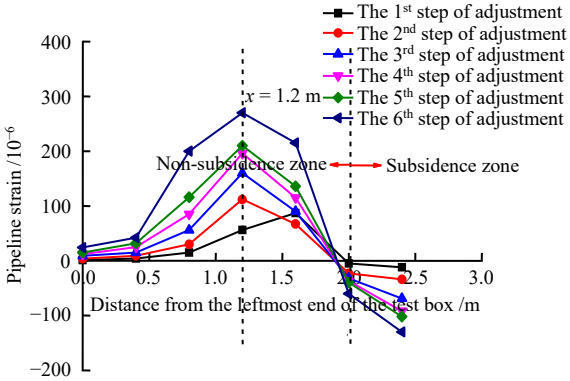

Fig. 17 Axial strain at the middle of the pipeline

tensile strain at the bottom occurred at the center line (x = 3 m) and the maximum compression strain was at x = 1.2 m.

After entering the complete subsidence stage, the maximum compression strains at the top and middle of the pipeline were 750×10^{-6} and 170×10^{-6}, which respectively increased by 36.3% and 112% compared with those in the partial subsidence stage, and the maximum tensile strains were 700×10^{-6} and 270×10^{-6}, which respectively increased by 112% and 28.6% compared with those in the partial subsidence stage. The maximum compression and tensile strains at the bottom were 700×10^{-6} and $1\,070\times10^{-6}$, respectively rising by 55.6% and 42.7% compared with those in the partial subsidence stage. It was thus concluded that the continued increase in subsidence displacement had a greater impact on the pipeline deformation compared to the subsidence zone expansion, with the maximum compression strain occurring at the center line of the pipeline top (x = 3 m), which was the critical failure plane of the pipeline in this cross section.

4.3 Effect of ground subsidence on the earth pressure around the pipeline

In the partial subsidence stage, the earth pressure above the pipeline was positive in the subsidence zone, and the earth pressure increment increased with the increase of the pipeline length (x = 2.4 m), and the maximum value appeared at the center line of the pipeline (x = 3 m). In the non-subsidence zone, the earth pressure was negative, and the increment first decreased and then increased as the pipeline length increased (x = 0 m) (see Fig. 18). The earth pressure in the lower and middle parts of the pipeline had the same trend. In the subsidence zone, the earth pressure was negative and the increment decreased with the increase of the pipeline length, and in the non-subsidence zone, the earth pressure was positive and the increment increased first and then decreased with the increase of the pipeline length, and the maximum value appeared at x = 1.2 m (see Figs. 19 and 20). Therefore, the pipeline was subject to a positive arching effect in the subsidence zone and a negative arching effect in the non-subsidence zone.

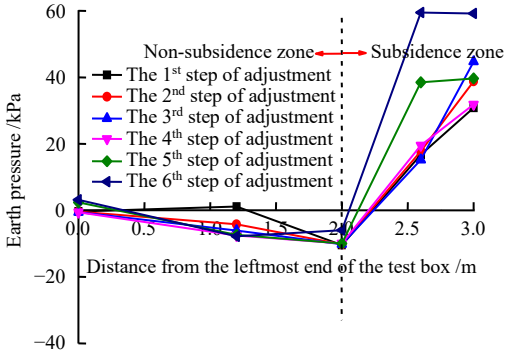

Fig. 18 Earth pressure distribution at the top of the pipeline

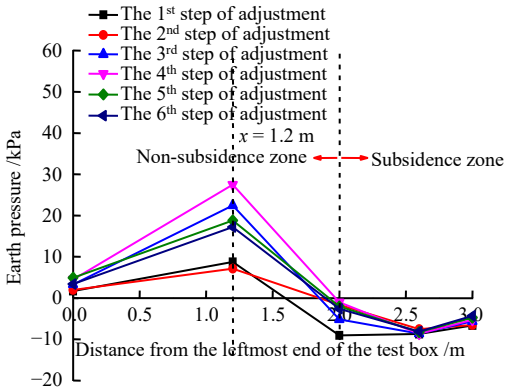

Fig. 19 Earth pressure distribution at the bottom of the pipeline

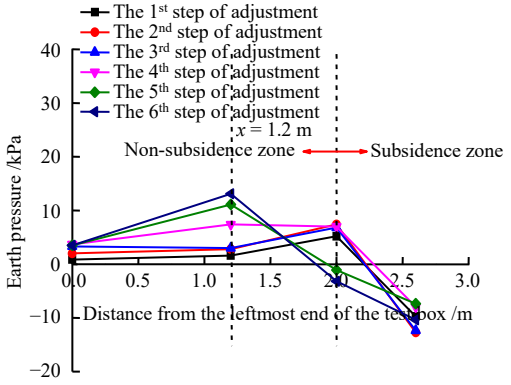

Fig. 20 Earth pressure distribution at the middle of the pipeline

In the complete subsidence stage, as the subsidence displacement increased, the maximum earth pressure at the top, middle and bottom of the pipeline increased to 59.2, 28 and 11.1 kPa, which increased by 32.4%, 24.4% and 50% respectively compared with those in the partial subsidence stage. The reason for this was that the pipeline had a restriction effect on the overlaying soil, and during the ground subsidence, the relative displacements of the overlaying soil above and around the pipeline gradually increased as the overlaying soil detached from the soil below the pipeline, and the arching effect led to a slow increase of the earth pressure in the subsidence zone. Thus, it could be concluded that after entering the complete subsidence stage, the earth pressure around the pipeline reached its peak value, and the pipeline was very prone to failure.

In order to investigate the effect of ground subsidence on the pipeline, the analysis for the earth pressure ratio λ was performed (see Fig. 21). During the partial subsidence stage, the earth pressure ratios at the top and middle of the pipeline gradually increased, indicating that the range of the pipeline tension area reduced while the range of the pipeline compression area gradually increased. After coming into the complete subsidence stage, the earth pressure ratio λ further increased, and the range of the compression area reached a peak at this time. The λ of the soil below the pipeline exhibited a trend of increasing

first and then decreasing during the ground subsidence.

5 Discussion

5.1 Effect of different settlement patterns on the earth pressure around the pipeline

The mechanical response of pipelines was significantly influenced by ground collapse and subsidence (see Figs. 22−24). The analysis showed that the earth pressure around the pipeline was less affected by the collapse compared to the ground subsidence. The earth pressure reached the peak value under the collapse effect after the 2nd step of adjustment of the ground collapse, and the maximum increments of the upper and lower earth pressure were 10.95 and 4.5 kPa, respectively, which only accounted for 24% and 16% of the corresponding zone after the 5th step of adjustment of the ground subsidence. After the 5th step of adjustment of ground collapse, the maximum earth pressure above and under the pipeline decreased

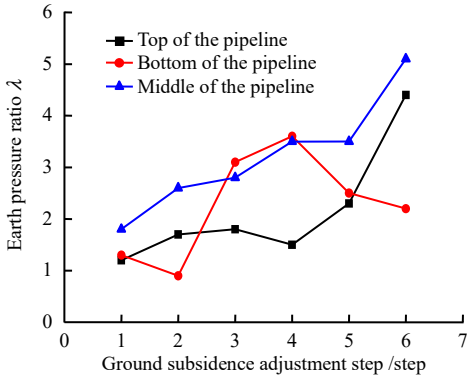

Fig. 21 Earth pressure ratio λ around the pipeline

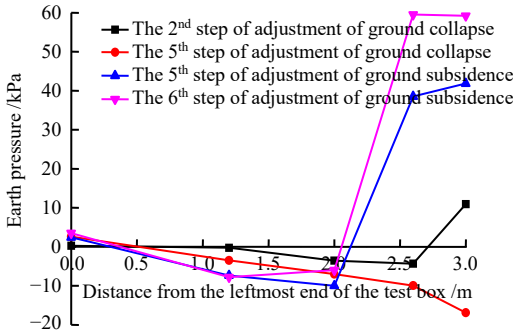

Fig. 22 Earth pressure distribution at the top of the pipeline

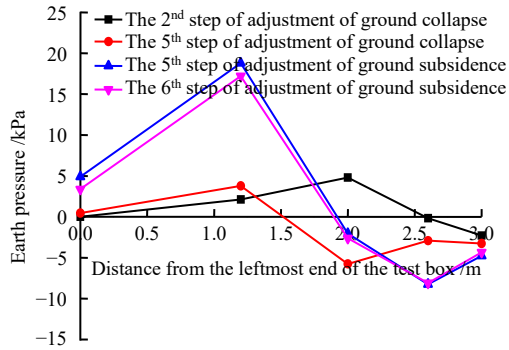

Fig. 23 Earth pressure distribution at the bottom of the pipeline

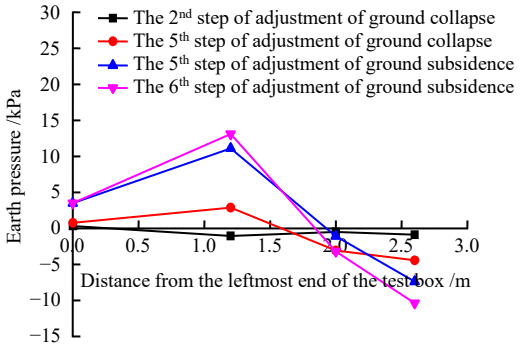

Fig. 24 Earth pressure distribution at the middle of the pipeline

sharply and the maximum earth pressure alongside the pipeline increased slightly as the overlaying soil collapsed. After the 6th step of adjustment of ground subsidence, the maximum earth pressure around the pipeline continued to increase as the subsidence displacement continuously increased. Thus, it was believed that the ground subsidence had a greater threat to the pipeline safety.

5.2 Calculation of vertical earth pressure at the top of the pipeline during ground subsidence

Under the influence of the arching effect, the earth pressure at the top of the pipeline varies significantly. Based on the modified Marston earth pressure model[25], the calculation method of vertical earth pressure at the top of the pipeline during the ground subsidence was developed (see Fig. 25). In this paper, the following assumptions were adopted: (1) the assumption of limit equilibrium; (2) the earth pressure at the top of the pipeline

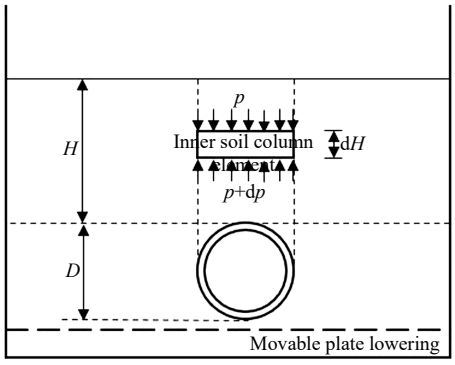

(a) Cross section analysis

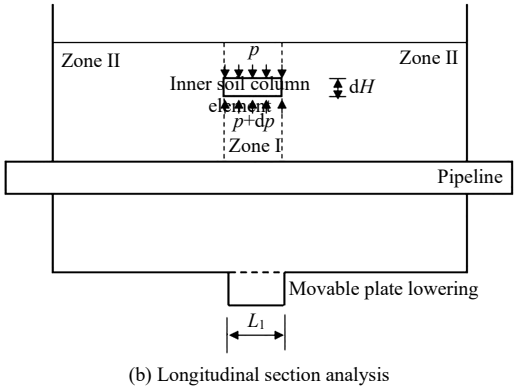

(b) Longitudinal section analysis

Fig. 25 Mechanical analysis for the pipeline

was assumed to be uniformly distributed (i.e., to ensure that the vertical earth pressure at the top of the pipeline was uniformly distributed in any plane along the depth direction); and (3) the pipeline embedment depth was assumed to be constant during the descent of the movable steel plate, i.e., the unit weight of the overlaying soil could be calculated after the stress redistribution.

Soil column element dH along the cross section direction of the pipeline top in the subsidence zone (zone I) was taken for analysis, and according to the vertical force equilibrium, one can obtain

$$Dp_1 + D\mathrm{d}p_1 = Dp_1 + \gamma D\mathrm{d}H + 2(\gamma_1 HK - 2c\sqrt{K}f + c)\mathrm{d}H \tag{1}$$

where D is the pipeline diameter (m); γ_1 is the soil unit weight (kN /m^3); p_1 is the vertical earth pressure at the pipeline top at depth H in the cross section analysis (kN /m^2); K is the earth pressure coefficient, $K = \tan(45^\circ - \varphi/2)$, φ is the internal friction angle of the backfilling soil; f is the friction coefficient, $f = \tan\varphi$; and c is the cohesion of the backfilling soil.

According to the displacement boundary condition of the pipeline end ($H = 0$, $p_1 = 0$), one can obtain

$$p_1 = \gamma_1 H + \frac{\gamma_1 H^2 Kf + 2c\left(1 - 2\sqrt{K}f\right)H}{D} \tag{2}$$

After adjusting the movable steel plate in the 1st step, the soil unit weight in the subsidence zone (zone I) was $\gamma_1' = p_1/H$, at this time, the dragging influence of soil outside pipeline on the overlaying soil above the pipeline was enhanced, and the soil column element dH along the longitudinal section direction of pipeline top in the subsidence zone was taken for force analysis. According to the vertical force equilibrium, one can get

$$L_1 p_1' + L_1\mathrm{d}p_1' + 2\left[\left(\gamma_1' HK - 2c\sqrt{K}\right)f + c\right]\mathrm{d}H = L_1 p' + \gamma_1' L_1 \mathrm{d}H \tag{3}$$

where L_1 is the width of the subsidence zone in the 1st step of adjustment; and p_1' is the vertical earth pressure at the depth H in the longitudinal section analysis (kN /m^2).

According to the displacement boundary condition of the pipeline end ($H = 0$, $p_1 = 0$), one can obtain

$$p_1' = \frac{\gamma_1' KfH^2 + (4c\sqrt{K}f - 2c)H}{L_1} + \gamma_1' L_1 \tag{4}$$

Transforming the partial earth pressure $p_1 - p_1'$ in the subsidence zone (zone I) to the non-subsidence zone (zone II), we get the earth pressure of the non-subsidence zone (zone II)

$$p_1'' = \gamma_1 H + \left(p_1 - p_1'\right) \tag{5}$$

After adjusting the movable steel plate in the 2nd step, the stress was redistributed at the top of the pipeline, the soil unit weight was $\gamma_2 = p_1''/H$. The cross section vertical earth pressure p_2 and longitude section vertical earth pressure p_2' at the pipeline top in the subsidence zone after the 2nd step of adjustment can be obtained by substituting γ_2 and the boundary condition ($H = 0$, $p_2 = 0$) into Eqs. (1) and (3). p_2 and p_2' are further substituted into Eq. (5) to obtain the vertical earth pressure at the pipeline top in the non-subsidence zone (zone II). Repeat the above steps until the earth pressure at the pipeline top was obtained after the 5th step of adjustment.

The pipeline and soil parameters in the model test (see Table 1) were substituted into the calculation formula, and compared with the earth pressure above the pipeline in the mid-span section, the results of the two were found to be consistent (see Table 2), which proved that the calculation formula was reliable.

Table 1 Parameters of the pipeline and foundation soil

Pipeline diameter /m	Embedment depth /m	Unit weight of soil /(kN • m^{-3})	Internal friction angle /(°)	Cohesion /kPa
0.076	0.8	15.2	27.5	0.5

Table 2 Comparison between calculation and experiment values of earth pressure at central line of top of pipeline

Adjustment step /step	Experiment value /kPa	Calculation value /kPa
1	28.30	30.84
2	33.25	28.79
3	38.80	44.73
4	41.42	39.64
5	51.95	41.83

6 Conclusion

Based on the self-developed large scale model box system, the mechanical response of buried pipelines under two settlement patterns (ground collapse and subsidence) was studied experimentally, and the formula for calculating the vertical earth pressure at the top of the pipeline during ground subsidence was proposed, and the main conclusions are summarized as follows:

(1) In the partial collapse stage, the soil below the pipeline in the collapse zone collapsed rapidly, but the overlaying soil still remained intact under the support of the pipeline, and the strain and earth pressure around the pipeline reached the peak value by the arching effect. In the collapse zone, the top of the pipeline was under pressure, and the bottom and middle of the pipeline were under tension. In the non-collapse zone, the top and middle of the pipeline were under tension, and the bottom of the pipeline was under pressure, and the center line of the pipeline top at $x = 3$ m (the maximum bearing strain) was the critical failure plane. In the complete collapse stage, the soil in the collapse zone collapsed and part of the soil in the non-collapse zone flowed out from the collapse zone. The elastic deformation of the pipeline gradually decreased with the reduction of the earth pressure around the pipeline.

(2) During the ground subsidence, the pipeline strain increased with the extension of the subsidence zone and the increase of the subsidence displacement. In the subsidence zone, the top and middle of the pipeline were under pressure and the bottom of the pipeline was under

tension. However, in the non-subsidence zone, the top and middle of the pipeline were under tension and the bottom of the pipeline was under pressure, and the maximum bearing strain was located at the center line of the pipeline top, and this section was the critical failure plane. Compared with the scenario of settlement zone extension, the pipeline strain was more significantly affected by the increase of subsidence. When the soil settled integrally another 50 mm, the maximum strain at the top, bottom and middle of the pipeline increased by 36.3%, 55.6% and 112%, respectively.

(3) In the partial collapse or subsidence stage, the earth pressure above the pipeline was positive and the earth pressure at the middle and bottom of the pipeline was negative due to the positive arching effect within the adjustment range. However, in the non-adjustment range, the earth pressure above the pipe was negative and the earth pressure at the middle and bottom of the pipeline was positive due to the negative arching effect. After entering the complete collapse or subsidence stage, the positive and negative arching effects weakened with the collapse of the overlaying soil, but further enhanced in the ground settlement process, and at this time, the ground settlement caused the pipeline bending deformation to reach the peak value , resulting in pipeline failure.

(4) Based on the modified Marston earth pressure model, the formula for calculating the vertical earth pressure at the top of the pipeline during ground settlement was developed. By comparing the earth pressure at the top of the pipeline in the model test, it could be found that the model test results were in better agreement with the theoretical solutions, so the calculation formula could be used to guide engineering practice.

Referneces

[1] LI Qiu-yang, ZHAO Ming-hua, REN Xue-jun, et al. Construction status and development trend of Chinese oil & gas pipeline[J]. Oil-Gas Field Surface Engineering, 2019, 38(Suppl.1): 14−17.

[2] HAN Bing, WANG Zhi-yin, WU Zhang-zhong, et al. Application of strain-based theory in failure analysis of pipeline subjected to mining collapse areas[J]. Journal of China University of Petroleum (Edition of Natural Science), 2012, 36(4): 134−138, 148.

[3] LIU Run, YAN Shu-wang, WANG Hong-bo, et al. Model tests on soil restraint to pipelines buried in sand[J]. Chinese Journal of Geotechnical Engineering, 2011, 33(4): 559−565.

[4] LIU Run, GUO Shao-zeng, WANG Hong-bo, et al. Soil resistance acting on buried pipelines in Bohai Bay soft clay[J]. Chinese Journal of Geotechnical Engineering, 2013, 35(5): 961−967.

[5] TANG Ai-ping, WANG Lian-fa, WU Bai-chao, et al. Centrifuge model test on a buried pipeline crossing reverse fault considering soil-structure interaction[J]. China Earthquake Engineering Journal, 2015, 37(3): 639−642.

[6] ZENG Xi, LEI Zhen, JIN Fang-qian, et al. Influence of different faults on stress performance of buried pipelines[J]. Oil & Gas Storage and Transportation, 2020, 39(1): 1−13.

[7] WANG F, DU Y J, YANG X. Physical modeling on ground responses to tunneling in sand considering the existence of HDPE pipes[J]. Geotechnical Testing Journal, 2015, 38(1): 85−97.

[8] O'ROURKE M, GADICHERLA V, ABDOUN T. Centrifuge modeling of PGD response of buried pipe[J]. Earthquake Engineering and Engineering Vibration, 2005, 4(1): 69−73.

[9] VORSTER T E, KLAR A, SOGA K, et al. Estimating the effects of tunneling on existing pipelines[J]. Journal of Geotechnical and Geoenvironmental Engineering, 2005, 131(11): 1399−1410.

[10] JU Yu-wen, WU Ji-yuan, HE Wu-bin, et al. Experimental study and numerical analysis on influence urban underground pipelines under the ground collapse[J]. Journal of Taiyuan University of Technology, 2015, 46(1): 64−68.

[11] WANG De-yang, ZHU Hong-hu, WU Hai-ying, et al. Experimental study on buried pipeline instrumented with fiber optic sensors under ground collapse[J]. Chinese Journal of Geotechnical Engineering, 2020, 42(6): 1125−1131.

[12] LIU Peng, HUANG Wei-he, LI Yu-xing, et al. Research on mechanical response of buried steel pipelines under continuous collapse[J]. Oil & Gas Storage and Transportation, 2021, 40(9): 1017−1026.

[13] WANG Wen, REN Jian-dong, DONG Miao, et al. A simulation experimental study on deformation evolution of natural gas pipeline under mining influence[J]. Journal of Mining & Safety Engineering, 2020, 37(4): 777−787.

[14] XU Ping. Study on the buried pipeline-soil interaction and its mechanical response by mining subsidence[D]. Xuzhou: China University of Mining and Technology, 2015.

[15] ZHOU Min, DU Yan-jun, WANG Fei, et al. Physical modeling of mechanical responses of HDPE pipes and subsurface settlement caused by land subsidence[J]. Chinese Journal of Geotechnical Engineering, 2016, 38(2): 253−262.

[16] ZHOU Min, DU Yan-jun, WANG Fei, et al. Mechanical response of buried HDPE pipes subjected to localized land subsidence[J]. Chinese Journal of Rock Mechanics and Engineering, 2017, 36(Suppl.2): 4177−4187.

[17] ZHOU M, WANG F, DU Y J, et al. Laboratory evaluation of buried high-density polyethylene pipes subjected to localized ground subsidence[J]. Acta Geotechnica, 2019, 14(4): 1081−1099.

[18] LIU Cheng-yu, CHEN Bo-wen, LIN Wei, et al. Prediction model for settlement caused by damage of underground pipelines and its experimental verification[J]. Chinese Journal of Geotechnical Engineering, 2021, 43(3): 416−424.

[19] LI Li-yun, ZUO Xiao, ZHONG Zi-lan. Size effect and reliability analysis of the model test for pipe-soil interaction[J]. Journal of Institute of Disaster Prevention, 2017, 19(2): 1−8.

[20] ZHANG Yu, HOU Zheng-sen, LI Da-yong, et al. Design and development of pipeline safety test platform under foundation settlement[J]. Experimental Technology and Management, 2021, 38(7): 135−140.

[21] China National Petroleum Corporation. GB 50251−2015 Code for design of gas transmission pipeline engineering[S]. Beijing: China Planning Press, 2015.

[22] WEI Chao, ZHU Hong-hu, GAO Yu-xin, et al. Model test study of ground collapse using distributed fiber optic sensing[J]. Rock and Soil Mechanics, 2022, 43(9): 2443−2456.

[23] CUI Peng-bo, ZHU Yong-quan, LIU Yong, et al. Model test and particle flow numerical simulation of soil arch effect for unsaturated sandy soil tunnel[J]. Rock and Soil Mechanics, 2021, 42(12): 3451−3466.

[24] ZHOU Xiao-wen, PU Jia-liu, BAO Cheng-gang. A study of the movement and failure characteristics of sand mass above the crown of a tunnel[J]. Rock and Soil Mechanics, 1999, 20(2): 32−36.

[25] MATYAS E L, DAVIS J B. Prediction of vertical earth loads on rigid pipes[J]. Journal of Geotechnical Engineering, 1983, 109(2): 190−201.